

Synchronization of Sacral Skin Blood Flow Oscillations in Response to Local Heating

Yih-Kuen Jan and Fuyuan Liao

Abstract—Local heating causes an increase in skin blood flow by activating sensory axon reflex and metabolic nitric oxide controls. It has been observed that the remote skin area without temperature changes also shows a slightly increase in blood flow. The responsible mechanism of this indirect vasodilation remains unclear. We hypothesized that the remote skin area will have enhanced synchronization of blood flow oscillations (BFO), thus inducing a vasodilatory response. We studied BFO in two sites separated 10cm of the sacral skin in 12 healthy people. Ensemble empirical mode decomposition method was used to decompose blood flow signals into a set of intrinsic mode functions (IMFs), and an IMF was selected to quantify each of myogenic, neurogenic, and metabolic modes of BFO. Then the instantaneous phase of the mode was calculated using the Hilbert transform. From the time series of phase difference between a pair of characteristic modes, we detected the epochs of phase synchronization and estimated the level of statistical significance using surrogate time series. The results showed that phase synchronization between neurogenic BFO was significantly higher in the period of the maximal vasodilation. We also observed a weak synchronization between myogenic BFO of the two skin sites. Our results suggested that synchronization of BFO may be associated with the changes in skin blood flow at the non-heated site.

I. INTRODUCTION

The study of skin microcirculation has been shown to be useful to assess risk for pressure ulcers [1-4]. Recently, skin blood flow response to local heat has been used to assess microvascular regulation using wavelet analysis [2, 5, 6]. These studies showed that metabolic nitric oxide is responsible for the maximal vasodilatory response and can be assessed by BFO in the frequency band at 0.0095-0.02 Hz. It is observed that the remote skin site without temperature changes also shows a slightly increase in skin blood flow (Fig. 1). Local heating applied at the sacral skin can induce a biphasic increase in blood flow (Fig. 1a) and a remote site (not under thermal stress) also shows a slightly increase in blood flow (Fig. 1b). The physiological mechanism responsible for this non-thermal induced vasodilation remains unclear. Based on our previous studies in BFO, we hypothesized that enhanced synchronization of BFO may be the responsible mechanism.

Manuscript received March 26, 2011. This work was supported in part by the National Institutes of Health (NIH) (R21HD065073) and the Oklahoma Center for the Advancement of Science and Technology (HR09-048).

Y. K. Jan is with the University of Oklahoma Health Sciences Center, Oklahoma City, OK 73117 USA (phone: 405-271-2131; fax: 405-271-242; e-mail: ykjan@ouhsc.edu).

F. Liao is with the University of Oklahoma Health Sciences Center, Oklahoma City, OK 73117 USA.

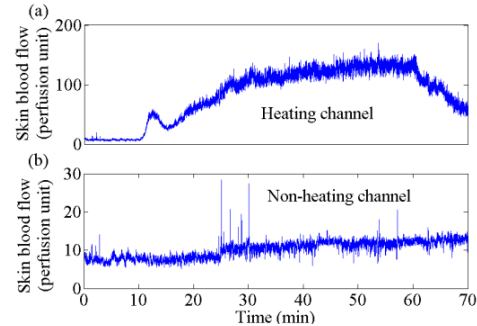


Fig. 1. Influence of local heat on skin blood flow at a nearby site. (a) A heating probe was used to heat the sacral skin to 42°C in 2 minutes and to maintain that temperature for 50 min, inducing a biphasic vasodilation. (b) At a site 10 cm horizontally lateral to the sacrum, skin blood flow showed a slightly increase.

BFO reflects five physiological control mechanisms of skin microcirculation, including cardiac, respiratory, myogenic, neurogenic, and metabolic activity [7, 8], with the corresponding frequency around 1 Hz, 0.2 Hz, 0.1 Hz, 0.04 Hz, and 0.01 Hz, respectively [7, 9]. It has been found that the heart and respiratory oscillations are synchronized [7, 10]. BFO generated by cardiac and respiratory systems are self-synchronized throughout the entire cardiovascular network [8]. For myogenic oscillations are only weakly self-synchronized [8].

Synchronization is a phenomenon that occurs when two or more nonlinear oscillators are coupled [10]. Phase synchronization means a certain relationship between the phases of interacting systems, while the amplitudes can remain uncorrelated [8]. The notion of synchronization has been used to analyze the interaction between physiological systems or subsystems, such as cardio-respiratory coupling [10] and cerebral blood flow regulation [11]. Different measures of synchronization have been proposed, including cross correlation or coherence function, mutual information, nonlinear interdependences, and phase synchronization [12, 13]. It was reported that these measures gave a similar tendency in synchronization levels [12, 13].

In this paper, we validate and develop an approach for detecting self-synchronization of myogenic, neurogenic, and metabolic BFO. It consists of three steps: extraction of the characteristic modes of BFO using the ensemble empirical mode decomposition (EEMD) method [14], calculation of the instantaneous phase of the modes using the Hilbert transform [15], and detection of phase synchronization epochs. Since the third step involves the choice of parameters [16], we tested the algorithm using the coupled Rössler systems.

II. MATERIALS AND METHODS

A. Experimental Data Sets

12 healthy subjects (age 25.3 ± 5.4 yrs (mean \pm standard deviation), 4 males and 8 females, body mass index 23.2 ± 2.4 kg/m²) were recruited into this study. Subjects were in a prone position for this experiment. A heating probe (Probe 415-242, Perimed AB, Sweden) was used to heat the sacral skin to 42°C in 2 minutes and to maintain that temperature for 50 min. Skin blood flow and skin temperature at the sacrum and a site 10 cm lateral to the sacrum were recorded by another laser Doppler flowmetry probe with a 32 Hz sampling rate.

B. Extraction of Characteristic Modes of BFO

The myogenic, neurogenic, and metabolic components are embedded in BFO, and therefore cannot be measured selectively. To extract these components, we applied the EEMD method [14] to blood flow signals. This technique is based on the assumption that any complicated data set consists of a finite and often small number of ‘intrinsic mode functions’ (IMFs) that admit well-behaved Hilbert transforms [17]. Each of these IMFs represents a frequency-amplitude modulation in a narrow band that can be related to a specific underlying process [17]. By visually inspecting the power spectra of the IMFs, one can easily select an IMF as the myogenic, neurogenic, or metabolic mode of BFO. Fig. 2 shows the obtained IMFs from the blood flow signal shown in Fig. 1(a) and their power spectra. In this example, the eighth IMF, ninth IMF, and tenth IMF are respectively chosen as myogenic, neurogenic, and metabolic modes.

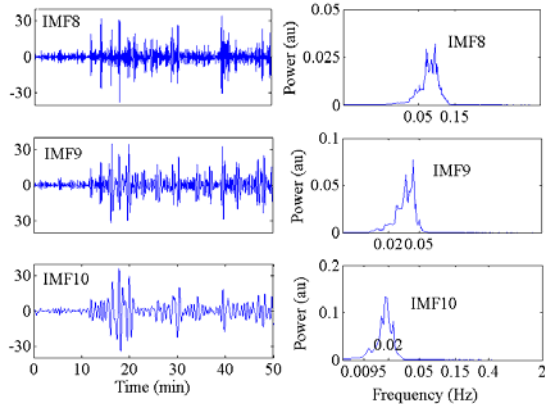


Fig. 2. Intrinsic mode functions (IMFs) obtained by the EEMD method and their power spectra. The original data is the blood flow signal shown in Fig. 1(a) during heating and recovery period (11-60 min). Here only the eighth IMF, the ninth IMF, and the tenth IMF are shown. By visually inspecting the power spectra of the IMFs, IMF8, IMF9, and IMF10 are respectively selected as myogenic, neurogenic, and metabolic modes.

C. Instantaneous Phase

From a characteristic mode of BFO, $x(t)$, the Hilbert transform can be used to construct an analytic signal, $z_x(t) = x(t) + i\tilde{x}(t) = A(t)e^{i\varphi(t)}$, where $\tilde{x}(t)$ is the Hilbert transform of $x(t)$, defined as [15]

$$\tilde{x}(t) = \frac{1}{\pi} p.v. \int \frac{x(\tau)}{t-\tau} d\tau, \quad (1)$$

where p.v. denotes the Cauchy principal value. The instantaneous phase is given by

$$\varphi(t) = \arctan \frac{\tilde{x}(t)}{x(t)}. \quad (2)$$

It should be noted that this method is reasonable only when the signal $x(t)$ has a narrow frequency band.

D. Algorithm for Detection of Phase Synchronization Epochs

For two characteristic modes of BFO, we consider the instantaneous phase difference

$$\Delta\varphi = \varphi_1 - \varphi_2, \quad (3)$$

where φ_1 and φ_2 are the unwrapped instantaneous phases of the two modes. The presence of 1:1 phase synchronization is defined by the condition $|\Delta\varphi| < \text{const}$ [18]. In this case, the phase difference $\Delta\varphi$ fluctuates around a horizontal plateau.

To detect the epochs of phase synchronization, we adopt the algorithm proposed by Karavaev *et al.* [16]. As illustrated in Fig. 3(a), for each time moment, t , the slope of the linear regression line, α , in the window $[t - \tau/2, t + \tau/2]$ is calculated. We thus obtain a time series consisting of such slopes (Fig. 3(b)). It should be noted that α is not defined for the initial and final regions of the time series of phase difference with the duration of $\tau/2$. Intuitively in a region of phase synchronization the phase difference fluctuates around a horizontal plateau, resulting in small values of $|\alpha|$. Therefore, an epoch is considered as a synchronization epoch if $|\alpha|$ is smaller than a threshold δ for all time moments in the epoch and the duration of the epoch exceeds T seconds.

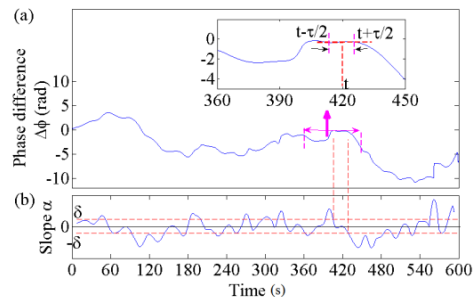


Fig. 3. Illustration of detection of the epochs of phase synchronization. (a) Phase difference between the neurogenic BFO of the heating channel (IMF9 in Fig. 2 during 51-60 min) and that of the non-heating channel. At each time moment, t , the slope of the linear regression line, α , in the window $[t - \tau/2, t + \tau/2]$ is calculated. It should be noted that α is not defined for the initial and final regions of the time series of phase difference with the duration of $\tau/2$. (b) The time series of α . An epoch is detected as a synchronization epoch if $|\alpha|$ is smaller than a threshold δ for all time moments in the epoch and the duration of the epoch exceeds T seconds.

The detected epochs of phase synchronization are dependent on the parameters, τ , δ , and T . Karavaev et al. [16] proposed that the choice of the parameters should be guided by the concept that the automatically detected epochs should be similar to those identified by visual inspection. The authors suggested the use the following parameters: τ is close to the characteristic period of oscillations, T is about one to two characteristic periods, and δ is about 0.005-0.01. However, we found that the parameter δ is dependent on the number of data points in one characteristic period of oscillations.

E. Simulation Study on Coupled Model Systems

To test the reliability of the above algorithm and investigate the dependence of the parameters, τ , δ , and T on the characteristic period of oscillations, let us consider two coupled Rössler systems [19]

$$\begin{aligned} \dot{x}_{1,2} &= -\omega_{1,2}y_{1,2} - z_{1,2} + C(x_{2,1} - x_{1,2}) \\ \dot{y}_{1,2} &= \omega_{1,2}x_{1,2} + 0.15y_{1,2} \\ \dot{z}_{1,2} &= 0.2 + z_{1,2}(x_{1,2} - 10), \end{aligned} \quad (4)$$

where the parameters $\omega_{1,2}=1\pm\Delta\omega$ control the frequency mismatch and the parameter C controls the strength of coupling [15]. We used $\omega_{1,2}=1\pm 0.1$ and C from 0 to 0.5 with a step of 0.01. The Rössler system has a narrow frequency band [13] and the instantaneous phase can be defined through the Hilbert transform [15]. To avoid time consuming in surrogate tests, the time series of phase difference was re-sampled to 8 Hz. Assuming that the characteristic frequencies of myogenic, neurogenic, and metabolic BFO are 0.1 Hz, 0.04 Hz, and 0.01 Hz, respectively [7, 9], the corresponded time series of phase difference have approximate 80 points, 200 points, and 800 points per cycle, respectively. Fig. 4 shows the phase difference of two coupled Rössler systems and the percentage of phase synchronization, s , for different coupling strengths C . The results indicate that the algorithm described in section D can reliably detect epochs of phase synchronization and that the parameter δ should decrease with the number of data points in one characteristic period of oscillations.

F. Application to Blood Flow Data

Skin blood flow at the heated site showed a biphasic response (Fig. 1a). The first peak is mediated by axon reflex mechanism and the second peak is mediated by nitric oxide mechanism [20]. Therefore, phase synchronization between two characteristic modes of BFO may be different in different periods. We employed the following steps.

(i) Detect all epochs of phase synchronization using the algorithm described in section D. For myogenic BFO, we used $\tau=6$ s, $\delta=0.015$, and $T=8$ s; for neurogenic BFO, we used $\tau=15$ s, $\delta=0.008$, and $T=20$ s; for metabolic BFO, we used $\tau=45$ s, $\delta=0.002$, and $T=60$ s.

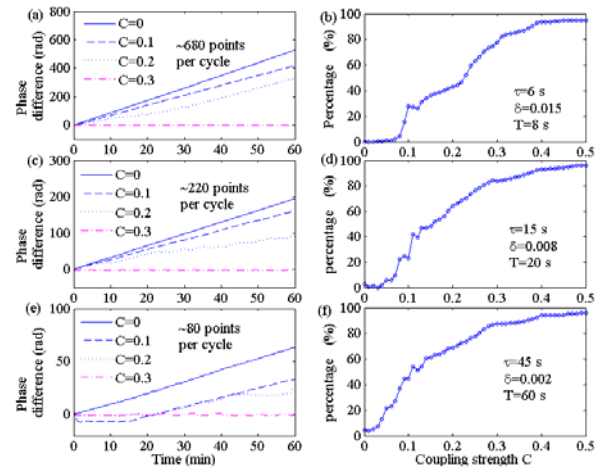


Fig. 4. Phase difference of two coupled Rössler systems (a, c, e) and the percentage of phase synchronization versus the strength of coupling (b, d, f).

(ii) Calculate the percentage of phase synchronization, s , in the following time intervals: 11-20 min, 21-30 min, ..., 51-60 min.

G. Estimation of Statistical Significance of Results

Because spurious phase synchronization can be detected even in the case of completely uncorrelated phases, we assessed the statistical significance of the obtained results using surrogate time series. First, for each of a pair of characteristic modes of BFO, we generated a surrogate time series by performing a Fourier transform on the mode, preserving the amplitudes of the Fourier transform but randomizing the phases, and then performing an inverse Fourier transform. Then the percentage of synchronization in the five time intervals was calculated. We repeated this procedure 1000 times and thus obtained a distribution, $P(s)$, of phase synchronization estimates for unsynchronized signals. As illustrated in Fig. 5, the level of statistical significance, p , for a percentage of phase synchronization, s_0 , calculated from experimental data was estimated as the ratio of the area under the distribution curve $P(s)$ corresponding to $s \geq s_0$ to the entire area under the distribution curve. When $p < 0.05$, the percentage of phase synchronization, s_0 , was considered to be statistically significant.

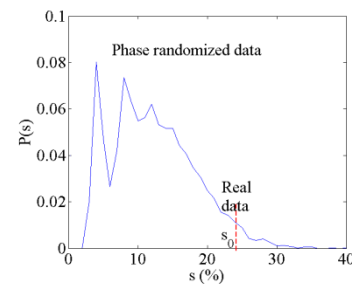


Fig. 5. Estimation of the level of significance of results calculated from real data. It is defined as the ratio of the area under the distribution curve $P(s)$ corresponding to $s \geq s_0$ to the entire area under the distribution curve. The real data is the time series of phase difference shown in Fig. 3(a).

III. RESULTS AND DISCUSSION

Fig. 6 (a) shows the normalized skin blood flow (normalized to the baseline) at the non-heated site. The results of percentage of phase synchronization of myogenic and neurogenic BFO as well as surrogate time series are shown in Fig. 6 (b), (c). Particularly, during 11-20 min, values of the percentage of phase synchronization, s , for either myogenic BFO or neurogenic BFO were comparable with that of surrogate data, indicating no phase synchronization existed in this period. On the contrary, during 51-60 min, values of s for neurogenic BFO were much higher than for surrogate data, and the level of statistical significance was lower than 0.05 in 10 subjects among the 12 subjects. In the other time intervals, i.e. 21-30 min, 31-40 min, and 41-50 min, although values of s were also higher for real data than for surrogate data, the differences were less significant. For metabolic BFO, We did not observe phase synchronization. The values of s for real data were comparable with those for surrogate data.

The observed flow increase at the non-heated site might also be due to other reasons, for example flow mediated dilation in an upstream larger vessel supplying both skin areas. To confirm our hypothesis, further studies may be needed. If local heating can induce an increase of blood flow in any skin area around the heated skin and there exists synchronization between BFO in the two skin areas, we may confirm that it is the synchronization that induces the vasodilatory response at the non-heated site.

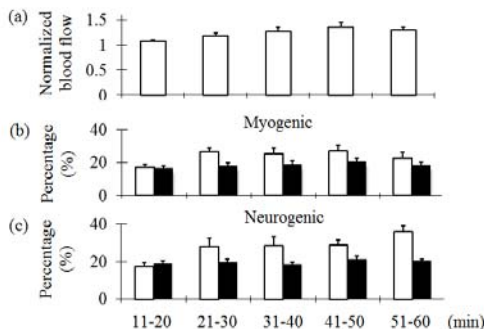


Fig. 6. (a) Normalized skin blood flow (normalized to the baseline) at the non-heated site. Values are means±SE. (b), (c) Percentage of phase synchronization for real data (blank bars) and surrogate data (filled bars). Values are means±SE. For each pair of myogenic or neurogenic modes of BFO, 1000 pair surrogate time series were generated.

IV. CONCLUSION

Our results indicated the existence of self-synchronization of myogenic and neurogenic BFO, which may be associated with an increase of skin blood flow at the non-heated site.

REFERENCES

- [1] Y. K. Jan, *et al.*, "Analysis of week-to-week variability in skin blood flow measurements using wavelet transforms," *Clinical Physiology and Functional Imaging*, vol. 25, pp. 253-262, Sep 2005.
- [2] Y. K. Jan, *et al.*, "Wavelet analysis of sacral skin blood flow oscillations to assess soft tissue viability in older adults," *Microvascular Research*, vol. 78, pp. 162-168, Sep 2009.
- [3] Y. K. Jan, *et al.*, "Wavelet-based spectrum analysis of sacral skin blood flow response to alternating pressure," *Arch Phys Med Rehabil*, vol. 89, pp. 137-45, Jan 2008.
- [4] Y. K. Jan, *et al.*, "Comparison of skin perfusion response with alternating and constant pressures in people with spinal cord injury," *Spinal Cord*, vol. 49, pp. 136-41, Jan 2011.
- [5] C. T. Minson, *et al.*, "Decreased nitric oxide- and axon reflex-mediated cutaneous vasodilation with age during local heating," *J Appl Physiol*, vol. 93, pp. 1644-9, Nov 2002.
- [6] A. Nicotra, *et al.*, "Heat-provoked skin vasodilatation in innervated and denervated trunk dermatomes in human spinal cord injury," *Spinal Cord*, vol. 44, pp. 222-6, Apr 2006.
- [7] A. Stefanovska and M. Bracic, "Physics of the human cardiovascular system," *Contemporary Physics*, vol. 40, pp. 31-55, Jan-Feb 1999.
- [8] A. Stefanovska and M. Hozic, "Spatial synchronization in the human cardiovascular system," *Progress of Theoretical Physics Supplement*, pp. 270-282, 2000.
- [9] A. Stefanovska, *et al.*, "Wavelet analysis of oscillations in the peripheral blood circulation measured by laser Doppler technique," *Ieee Transactions on Biomedical Engineering*, vol. 46, pp. 1230-1239, Oct 1999.
- [10] C. Schafer, *et al.*, "Heartbeat synchronized with ventilation," *Nature*, vol. 392, pp. 239-40, Mar 19 1998.
- [11] V. Novak, *et al.*, "Multimodal pressure-flow method to assess dynamics of cerebral autoregulation in stroke and hypertension," *Biomed Eng Online*, vol. 3, p. 39, Oct 25 2004.
- [12] R. Q. Quiroga, *et al.*, "Performance of different synchronization measures in real data: A case study on electroencephalographic signals," *Physical Review E*, vol. 65, pp. -, Apr 2002.
- [13] T. Kreuz, *et al.*, "Measuring synchronization in coupled model systems: A comparison of different approaches," *Physica D-Nonlinear Phenomena*, vol. 225, pp. 29-42, Jan 1 2007.
- [14] Z. H. Wu and N. E. Huang, "Ensemble empirical mode decomposition: A noise assisted data analysis method," Center for Ocean-Land-Atmosphere Studies, Calverton, MD, USA 2005.
- [15] M. G. Rosenblum, *et al.*, "Phase synchronization of chaotic oscillators," *Physical Review Letters*, vol. 76, pp. 1804-1807, Mar 11 1996.
- [16] A. S. Karavaev, *et al.*, "Synchronization of low-frequency oscillations in the human cardiovascular system," *Chaos*, vol. 19, p. 033112, Sep 2009.
- [17] N. E. Huang, *et al.*, "The empirical mode decomposition and the Hilbert spectrum for nonlinear and non-stationary time series analysis," *Proceedings of the Royal Society of London Series a-Mathematical Physical and Engineering Sciences*, vol. 454, pp. 903-995, Mar 8 1998.
- [18] P. Tass, *et al.*, "Detection of $n : m$ phase locking from noisy data: Application to magnetoencephalography," *Physical Review Letters*, vol. 81, pp. 3291-3294, Oct 12 1998.
- [19] O. E. Rossler, "Equation for Continuous Chaos," *Physics Letters A*, vol. 57, pp. 397-398, 1976.
- [20] B. L. Houghton, *et al.*, "Nitric oxide and noradrenaline contribute to the temperature threshold of the axon reflex response to gradual local heating in human skin," *J Physiol*, vol. 572, pp. 811-20, May 1 2006.